Progress In Electromagnetics Research M, Vol. 33, 121–135, 2013

HYBRID FEM-FMM APPROACH FOR EFFICIENT CALCULATIONS OF PERIODIC PHOTONIC STRUCTURES

Alexander Dorodnyy[1, *], Valery Shklover[2], and Christian Hafner[1]

[1]ETH Zurich, Institute of Electromagnetic Fields (IFH), Zurich 8092, Switzerland

[2]ETH Zurich, Laboratory of Crystallography, Zurich 8093, Switzerland

Abstract—A hybrid approach to find the optical response of periodic photonic structures to incident light is presented. The approach is based on a scattering matrix combination of the Finite Element Method (FEM) and the Fourier Modal Method (FMM). Optical response calculations include: scattering in both reflection and transmission directions, absorption and electric and magnetic field distributions inside the structure. The approach is tested on a structure — composed of dielectric and metallic materials — that is periodic in one direction. An analysis of the calculation accuracy shows that the approach depends on the subdivision into FEM and FMM domains and that the optimal subdivision depends on the calculations frequency range as well as on the structure geometry. For testing, we use the commercial FEM solver contained in CST Microwave Studio and a based on C/C++ Fourier Modal Method implementation.

1. INTRODUCTION

There are many methods for solving electromagnetic problems: Finite Element Method (FEM) [1], Fourier Modal Method (FMM) [2–4], Multiple Multipole Program (MMP) [5–7], Finite Difference Time Domain (FDTD) [8, 9], Boundary Element Method (BEM) [10, 11] and others.

Among them, one of the most widely used ones is the FEM. This is an extremely flexible method used in many different areas, such as interaction of light with periodic gratings [12], carrier transport

Received 23 August 2013, Accepted 23 September 2013, Scheduled 14 October 2013

* Corresponding author: Alexander Dorodnyy (dorodnya@ethz.ch).

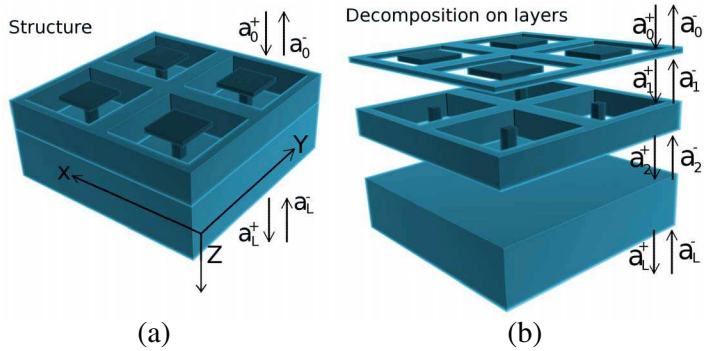

Figure 1. (a) Example of a periodic structure and (b) its FMM decomposition into layers which are homogeneous along the "Z" direction.

in semiconductors [13], heat transfer [14], acoustics [15] etc.. In the present work we investigate scattering of light by infinite periodic photonic structures (periodic in one or two dimensions in the plane perpendicular to "Z" axis in Figure 1). The incident light is directed from top to bottom (positive direction of "Z" axis). In the frame mentioned above, FEM has one considerable disadvantage in comparison with some other methods: the FEM simulation time grows super-linearly with the unit cell volume of the scattering structure. This occurs due to a linear growth of the number of degrees of freedom with the unit cell volume and the super-linear dependence of the simulation time from the number of degrees of freedom.

Among the methods listed above FMM, MMP and BEM do not have this drawback. MMP and BEM are based on boundary discretization. Therefore, their simulation time depends on the size of the boundaries to be discretized. FMM, as indicated by its name, is based on the expansion of the electromagnetic field into Fourier harmonics which is favorable for periodic structures. It will be explained later that the biggest drawback of FMM is the necessity to divide the unit cell into layers cylindrical along "Z" axis[†] (see Figure 1). This leads to long FMM simulation times for "complicated" geometries (such as spherical objects) that must be approximated by many short cylindrical slices. However, a big advantage of FMM is that the simulation time for cylindrical sections within the unit cell does not depend on their volume. For example, if we stretch the unit cell in "Z" direction by a factor F, the FEM simulation time grows more than F times while the FMM simulation time remains almost

[†] By cylindrical we understand layers with translational symmetry along "Z".

the same.

These advantages and disadvantages of FEM and FMM methods lead to the natural idea of merging the two techniques in order to get rid of their drawbacks, i.e., "long sections" shall be modeled by FMM and "complicated geometries" by FEM. The hybridization of FMM and FEM can be achieved by the scattering matrix (S-matrix) approach. This is convenient for two main reasons: 1) The approach is universal and not limit to the combination of FEM and FMM, i.e., it could be used for almost any pair of methods, e.g., MMP and FEM, BEM and FEM. 2) The S-matrix is already a natural part of FMM and is computed automatically with every FMM calculation.

To test the concept of the hybrid approach, we used CST Microwave Studio for the FEM part and our own implementation of FMM based on C/C++. In order to compute the scattering matrix with CST Microwave Studio for the FEM part we use its Matlab interface and a matrix assembling script. In Section 2 we illustrate the advantages and disadvantages of the methods using a rather simple 2D example that is periodic in one direction. In Sections 3 and 4 a detailed analysis of the hybrid approach is given.

2. FMM AND FEM

The Fourier Modal Method in application to periodic structures is based on the decomposition of Maxwell equations into one- or two-dimensional Fourier series. The dimensionality of the Fourier series depends on the number of periodic symmetries of the structure. In Figure 1 a photonic structure periodic in 2 directions is shown. The Fourier decompositions in this case should be done along "X" and "Y" directions, while the structure needs to be split into layers along the "Z" direction for the FMM analysis. Note that these layers are homogeneous in "Z" direction. Note also that both FEM and FMM work in frequency domain, i.e., no time analysis is required for combining FEM and FMM.

Figure 1 shows incoming (a_0^+, a_L^-), outcoming (a_L^+, a_0^-) and internal (a_1^+, a_1^-, a_2^+, a_2^-) Fourier modes. The corresponding amplitudes are connected to each other through a scattering matrix:

$$\begin{pmatrix} a_L^+ \\ a_0^- \end{pmatrix} = S \cdot \begin{pmatrix} a_0^+ \\ a_L^- \end{pmatrix} \tag{1}$$

$$\begin{pmatrix} a_n^+ \\ a_{n-1}^- \end{pmatrix} = S_n \cdot \begin{pmatrix} a_{n-1}^+ \\ a_n^- \end{pmatrix} \tag{2}$$

Here S is scattering matrix of the whole structure and S_n a scattering matrix of the layer $n \in [1, L]$ (number of layers: $L = 3$ in Figure 1).

Scattering matrices of individual layers S_1–S_L could be used to compute the scattering matrix S of the structure. One should be aware of the fact that the modes in Equations (1), (2) are vector quantities composed of two sets of Fourier harmonics corresponding to two light polarizations. Modes of incoming light, for example, are plane waves with k-vector components in "X" and "Y" directions defined by the corresponding Fourier order. To understand how modes that propagate inside the structure work (see Figure 1 on the right) one needs to start with the Fourier expansion of electric and magnetic fields[‡]:

$$\vec{E}(\vec{r}) = \sum_{q=0}^{n_x} \sum_{j=0}^{n_y} \vec{E}_{qj} e^{i\left(G_x^q + k_x\right)x + i\left(G_y^j + k_y\right)y} \tag{3}$$

$$\vec{H}(\vec{r}) = \sum_{q=0}^{n_x} \sum_{j=0}^{n_y} \vec{H}_{qj} e^{i\left(G_x^q + k_x\right)x + i\left(G_y^j + k_y\right)y} \tag{4}$$

Here G_x^q and G_y^j correspond to the structure periodicity (for example, $G_x^q = \frac{2\pi}{d_x} \cdot n_q$ where $n_q \in \mathbb{Z}$ corresponds to periodic properties of mode number q along "X", where d_x is the period in "X" direction), k_x and k_y are x and y components of the k-vector of the incident light. After substituting that into Maxwell equations one can get:

$$\left(\mu k_0^2 \frac{\partial^2}{\partial z^2} + FG\right) \begin{pmatrix} E_0^x \\ E_1^x \\ \dots \\ E_{N-1}^x \\ E_0^y \\ E_1^y \\ \dots \\ E_{N-1}^y \end{pmatrix} = 0 \tag{5}$$

$$F = \begin{pmatrix} K_x \epsilon^{-1} K_y & \mu k_0^2 - K_x \epsilon^{-1} K_x \\ K_y \epsilon^{-1} K_y - \mu k_0^2 & -K_y \epsilon^{-1} K_x \end{pmatrix} \tag{6}$$

$$G = \begin{pmatrix} -K_x K_y & K_x^2 - \mu k_0^2 \epsilon \\ \mu k_0^2 \epsilon - K_y^2 & K_x K_y \end{pmatrix} \tag{7}$$

Here K_x, K_y and ϵ are matrices (K_x, K_y are composed of k-vector components of different Fourier harmonics and ϵ is composed of Fourier harmonics of the permittivity) and $k_0 = \frac{\omega}{c}$ where ω is a frequency of the incident light. Since the medium is homogeneous in "Z" direction within each layer, the second derivative in Equation (5) will become

[‡] For detailed information see [2].

$-k_z^2$ where k_z is a propagation constant in the "Z" direction (in the corresponding layer):

$$\left(\mu k_0^2 k_z^2 - FG\right) \begin{pmatrix} E_0^x \\ E_1^x \\ \cdots \\ E_{N-1}^x \\ E_0^y \\ E_1^y \\ \cdots \\ E_{N-1}^y \end{pmatrix} = 0 \tag{8}$$

The mode amplitudes shown in Figure 1(b) correspond to eigenmodes calculated from Equation (8). Now, one has to find a connection between mode amplitudes and amplitudes of electric and magnetic field components. From Equation (8) we can find k_z and the field components E_x and E_y of each mode. For obtaining the components of the magnetic field we can use the Maxwell equations:

$$\begin{pmatrix} E_0^x \\ \cdots \\ E_{N-1}^x \\ E_0^y \\ \cdots \\ E_{N-1}^y \\ H_0^x \\ \cdots \\ H_{N-1}^x \\ H_0^y \\ \cdots \\ H_{N-1}^y \end{pmatrix} = \begin{pmatrix} \Psi e^{iK_z z} & \Psi e^{-iK_z z} \\ \frac{1}{\mu k_0} G K_z^{-1} \Psi e^{iK_z z} & -\frac{1}{\mu k_0} G K_z^{-1} \Psi e^{-iK_z z} \end{pmatrix} \begin{pmatrix} a_0^+ \\ \cdots \\ a_{2N-1}^+ \\ a_0^- \\ \cdots \\ a_{2N-1}^- \end{pmatrix} \tag{9}$$

Here Ψ is a matrix composed of eigenvectors found from Equation (8). K_z is a diagonal matrix that contains eigenvalues in the order corresponding to Ψ. The variable z is the distance along the "Z" axis between the plane where we calculate field amplitudes ($E_j^{x/y}$, $H_j^{x/y}$) and the plane where the mode amplitudes ($a_j^{+/-}$) are defined. One should also mention that the number of modes is twice the number of Fourier harmonics because of two polarizations of light.

For each layer one can define and calculate a scattering matrices (for example, the matrix S_2 connecting (a_1^+, a_2^-) and (a_1^-, a_2^+) modes, see Figure 1). Then all scattering matrices S_n are merged into the scattering matrix S of the whole structure. From the linear system of equations that connects modes on different sides of all layers we exclude

Figure 2. Depiction of photonic structure, (a) decomposed on layers for FMM, (b) meshed with FEM (CST Microwave studio), (c) top part FEM/bottom part FMM.

all internal modes and leave only incoming and outcoming ones. It is more convenient to merge layers one by one: first merging the first and second layers than merge third with them and so on [16]. For structures containing elements that are not piecewise cylindrical such as the one in Figure 2, FMM requires to split the structure into sufficiently thin layers (mostly to accomodate the shape of non-cylindrical elements). For a good performance, the number and thicknesses of the layers should be adjusted according to the shape and material dispersion of different elements of the structure. For example, metallic shapes may require more layers than the same shapes made of dielectric materials. If we need to describe a sphere by splitting it into layers, it is reasonable for a good FMM performance to split the sphere into layers with unequal thicknesses making them denser close to top and bottom of the sphere[§].

The Fourier Modal Method is fast for piecewise cylindrical structures with not many layers. For each layer the performance of the method depends very weakly on its thickness. The Finite Element Method is suitable for arbitrary geometries, but it is sensitive to the unit cell volume of a structure (thickness of each individual layer), i.e., it is inefficient for thick cylindrical layers. In Figure 2 three variants of solving the same structure are illustrated. Variant (a) is to solve the entire structure using FMM. This will cause a long computation time due to the non-cylindrical shape of the top part of the structure. Variant (b) is to solve the entire structure with FEM, which in its turn will cause long computation time of the bottom part of the structure because the FEM computation time is volume dependent. An improved solution is shown in Figure 2(c): calculating S-matrix for the top part with FEM; calculating S-matrix for the bottom part

[§] If a sphere is contained in a homogeneous medium, one only needs to explicitly calculate the scattering matrix for the top half of the sphere. Then one can flip it to obtain the scattering matrix for the bottom half and merge the two S-matrices.

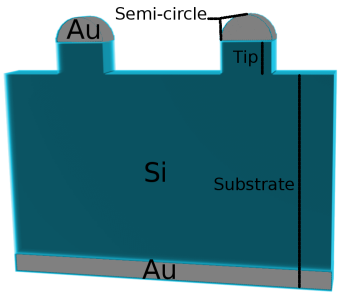

Figure 3. Sample photonic structure periodic in one dimension. Structure parameters: period — 860 nm, silicon bulk layer thickness — 1000 nm, silicon tips hight — 160 nm, golden underlayer thickness — 100 nm, golden semi-circles radius — 130 nm.

with FMM and merging the two S-matrices. That will decrease computation time while preserving the accuracy of the simulation. Note that one may also have several "FEM" sections separated by several FMM sections.

For reasons of simplicity we now consider the relatively simple structure that is periodic in one dimension, shown in Figure 3. Despite of its geometric simplicity, the structure has some features that cause numerical problems. The metallic half-circles on top of silicon tips have sharp edges and triple-points of metal-silicon-air contacts, which may cause significant FMM errors because of strong local fields. Calculations of spectra at normal light incidence for two polarizations (TE, where the electric field is perpendicular to the direction of the periodicity and TM, where the magnetic field is perpendicular to the direction of the periodicity) were performed for the whole structure with both FEM and FMM (i.e., the variants (a) and (b) illustrated in Figure 2). Results are shown in Figure 4. As one can see, one has a rather good agreement for the TE case, whereas the TM case is more demanding and would require a finer FMM discretization.

For testing the hybrid approach we focus on the more problematic TM case. To make sure that FMM is responsible for the bad agreement in Figure 4, spectra of the reflection of zero and first order modes are plotted for only the top gold part of the structure in Figure 5. We see that the FMM solution has considerable oscillations in the TM polarizations in both reflection orders. These oscillations are due to the high field intensity near the edges of the semi-circles. It is difficult to avoid them even with relatively high order Fourier modes in FMM (91 modes were used for the calculations shown in Figures 4 and 5).

In the following sections, the hybrid approach will be formulated

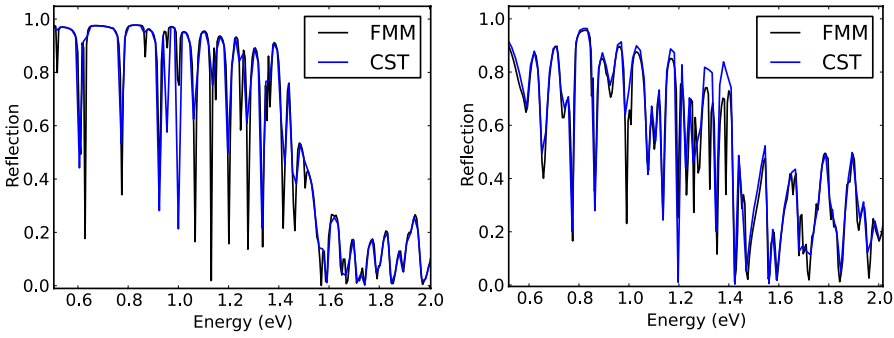

Figure 4. Comparison of pure FMM and FEM computations for the structure shown in Figure 3 for normal incidence. Zero-order mode reflection spectra are shown for (a) TE and (b) TM polarizations.

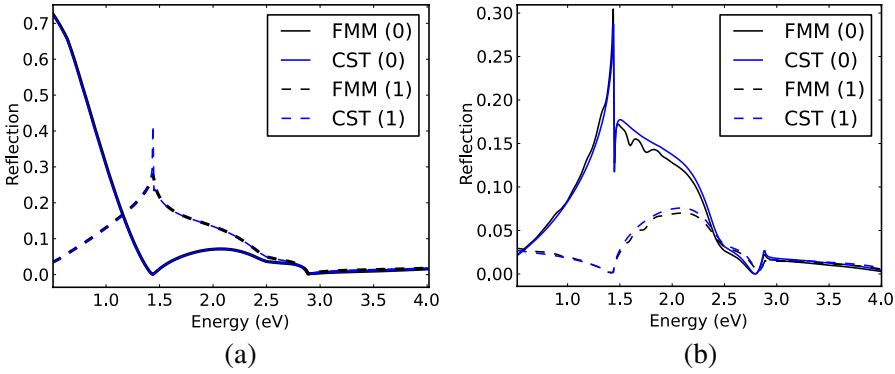

Figure 5. The reflection spectra of golden semi-circles for the zero and first order modes for (a) TE and (b) TM polarizations.

and applied to the test structure (see Figure 3) with subsequent analysis of the accuracy. Before that, we should mention that: 1) all FMM calculations were performed for 91 modes, therefore the scattering matrix size was 364×364, 2) to accelerate FEM calculations only 52 modes in the S-matrix were actually calculated with FEM while the rest were filled with zeros (this was done to accelerate FEM computations, because the FEM accuracy does not depend on the number of modes), 3) each calculation was performed over 300 equidistant frequency points in the range between 0.5 and 4 eV.

3. CUTTING PLANE POSITIONS BETWEEN FEM AND FMM

To start model assembling with the hybrid approach one needs first to decide which regions are to be solved with FEM and which ones are to be calculated with FMM.

In Figure 6 a sample structure is shown. There are two regions which could be better solved with FEM: 1) between A2 and A3, 2) below A5. Cutting plane positions A1–A5 are the natural ones, they are located at jumps of material properties. If one would solve the whole structure with FMM, A1–A5 would be borders between different layers and the areas between A2 and A3 and below A5 would be further subdivided. A natural way to define regions for FEM would be to use for FEM section between A2 and A3 and one below A5. In general this is not an optimal decision in terms of accuracy of the hybrid approach. It will be shown in the next section that one can benefit from arbitrary cutting planes (B1–B3 in Figure 6). In this case, regions between B1 and B2 and below B3 will be solved with FEM. The optimal positions of B1–B3 depend on the material properties and excitation parameters, as we will demonstrate in the following. An example of the optimization of the cutting plane position is shown in the next section on the simple test case.

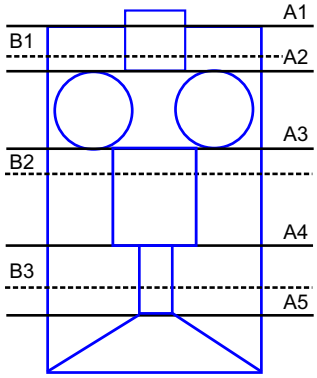

Figure 6. Example of natural (A1–A5) and arbitrary (B1–B3) positions of the cutting planes for a sample structure.

4. HYBRID APPROACH

To implement the hybrid approach, one must be able to compute the scattering matrix with FEM. For this purpose we have used the Matlab

interface of CST Microwave studio, which allows us to automatically calculate the optical response of the system for different modes of incident light[‖] (i.e., the FEM part S-matrix). A factor that has a considerable impact on the accuracy of these calculations is the position of the cutting planes that divide regions calculated by FEM and by FMM. The cutting plane positions should be chosen in such a way that the solution has a field that is as homogeneous as possible along all cutting planes. Although the field is not known before the simulations have been performed, one can make an analytical estimation or rough numerical simulation for the field profile. In the test example, we want to focus FEM calculations on the semi-circular part of the structure. Thus, only one cutting plane is required. There are two natural positions where one can place such a plane: right below the golden semi-circles and right below the silicon tips. One, however, can not be sure that any of these two "natural" positions will be optimal and one can assume that some position in between would be better. For this reason we investigate the dependence of the hybrid approach accuracy on the distance of the cutting plane form the semi-circles flat side (z_c). We performed calculations with the distance starting from 0 to 160 nm with 10 nm steps. The calculation error was estimated according to the equations below for the zero order reflection amplitude "A_0" in relation to an accurate FEM reference solution "A_0^{ref}":

$$\delta R_0(\omega, z_c) = \left(A_0(\omega, z_c) - A_0^{ref}(\omega)\right)^2 \tag{10}$$

$$\Delta R_0(z_c) = \int \delta R_0(\omega, z_c) d\omega / (\omega_{\max} - \omega_{\min}) \tag{11}$$

$$R_0^c(z_c) = \int \omega \delta R_0(\omega, z_c) d\omega / \Delta R_0(z_c) \tag{12}$$

$$\overline{R_0}(\omega) = \frac{\sum_{z_c} \delta R_0(\omega, z_c)}{\text{number of } z_c \text{ positions}} \tag{13}$$

Here we define several quantities describing the accuracy of the simulations: $\Delta R_0(z_c)$ is the square error average over the frequency, $R_0^c(z_c)$ is the position of the square error mass center on a frequency scale and $\overline{R_0}(\omega)$ is the error average over all z_c values.

The distribution of $\overline{R_0}$ over the frequency is shown in Figure 7. The error curve has sharp peaks in the area from 0.5 to 2.5 eV, where

[‖] One has to be careful with mode amplitudes in different software packages and make sure that they correspond to the same physical meaning. i.e., the Ψ matrices that define the relation between modes and field amplitudes should be the same in both FEM and FMM solvers.

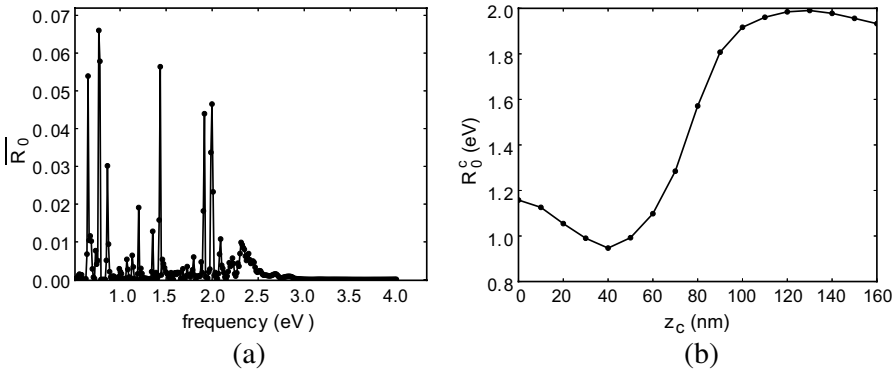

Figure 7. (a) $\overline{R_0}(\omega)$ and (b) $R_0^{\omega}(z_c)$.

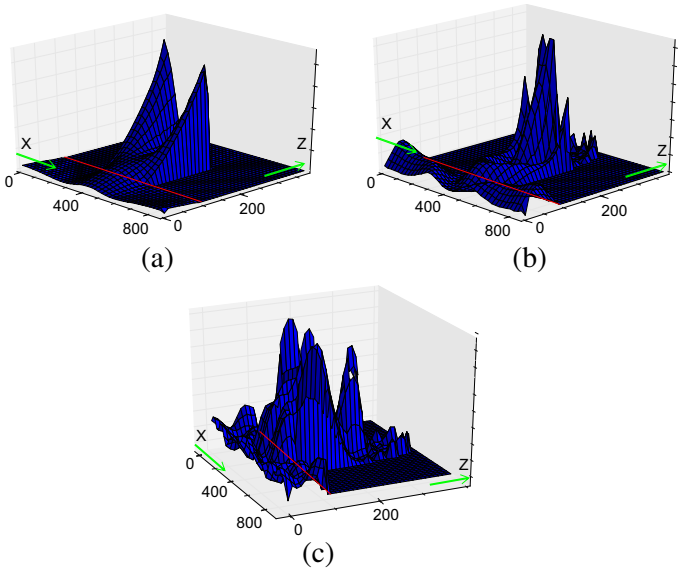

Figure 8. Distributions of the absolute value of the electric field for: (a) 0.76 eV, (b) 1.50 eV and (c) 2.00 eV. The silicon tip/substrate border corresponds to the value 100 nm on the "Z" axis (red lines).

the structure has multiple resonances. We can see that the frequency mass center R_0^c of the error shifts with displacement of the cutting plane from lower to higher frequencies due to a shift in the electric field distributions. In Figure 8 it is shown that the electric field has a sharp jump on the metal-dielectric border at lower frequencies. This is caused by plasmon resonance. At higher frequencies resonances related

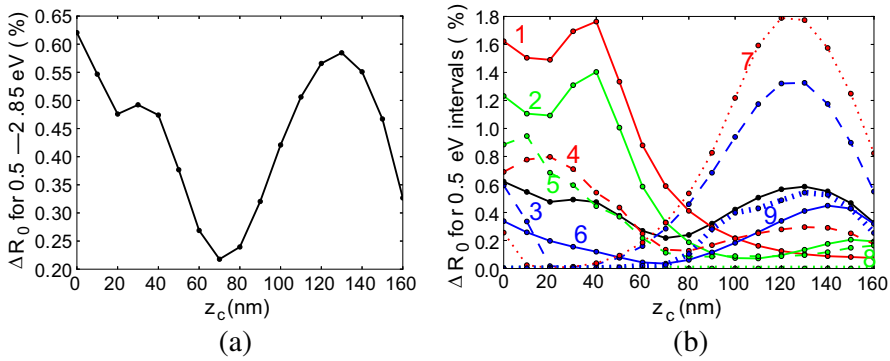

Figure 9. (a) ΔR_0 curves for broad frequency range and (b) 0.5 eV intervals. Black line 0) is the same as in the left figure. Frequency intervals for lines: 1) 0.5–1.0 eV, 2) 0.75–1.25 eV, 3) 1.0–1.5 eV, 4) 1.2–1.7 eV, 5) 1.4–1.9 eV, 6) 1.7–2.2 eV, 7) 1.9–2.4 eV, 8) 2.1–2.4 eV, 9) 2.35–2.85 eV).

to the periodicity come into play, shifting the biggest inhomogeneity in the field towards the border between the substrate and the silicon tips. That explains why we observe a R_0^c shift with changing z_c. When the cutting plane is close to the metal-dielectric border we observe the biggest error for lower frequencies, because the field has sharp changes near the metal-dielectric contact at these frequencies.

To decide which position of the cutting plane gives the lowest error for the hybrid approach, we performed calculations of ΔR_0 over a broad frequency interval and overlapping 0.5 eV intervals (Figure 9).

From Figure 9 we can see that the error has a minimal value for the cutting plane located close to the center of the silicon tip ($z_c = 80$ nm). For positions closer to the border of the golden semi-circles the error grows at lower frequencies and if the cutting plane shifts toward the substrate, the error grows for higher frequencies. This observation is valid for the chosen frequency interval. For calculations from 0.5 to 1.0 eV only it is more reasonable to place the cutting plane close to the substrate. This means that the optimal position of the cutting plane depends on both the structure and the considered frequency range.

Figure 10 shows a comparison of the hybrid approach calculations for the zero-mode reflection with FEM and FMM. The hybrid approach was calculated here with the cutting plane close to the middle of the silicon tips (which is optimal position as we found earlier). The hybrid approach reproduces results obtained with FEM (Figure 10(b)) and the accuracy is better than FMM alone (Figure 10(a)).

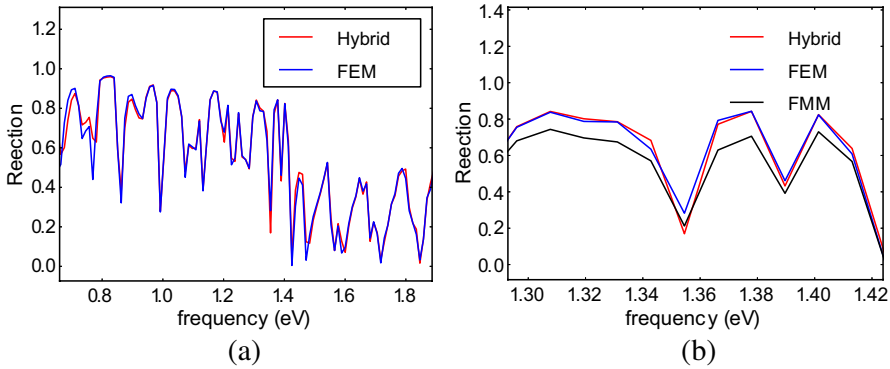

Figure 10. Comparison of results obtained by the hybrid approach (a) with both FEM and FMM on a closer scale and (b) with FEM.

5. CONCLUSIONS

A hybrid FEM-FMM approach is described and applied to the simulation of a periodic structure with semi-circular gold structures on a grated silicon layer. The simulations revealed that the hybrid approach is more accurate than a pure FMM due to a better accuracy of FEM especially for the semi-circular structure parts. At the same time, the hybrid approach utilizes an advantage of FMM in calculations of bulky structures, which reduces the computation time. When sufficiently long cylindrical sections are presented.

To make a S-matrix connection between FEM and FMM, one has to derive a scattering matrix from the FEM simulations. This requires extended calculation time, but the scattering matrix of a layer only needs to be calculated once. After this the FEM S-matrix could be combined with various scattering matrices of the environment computed with FMM (or another numerical method). Choosing the position of cutting plane that divide FEM and FMM regions should be done in a way that the field along this plane is as homogeneous as possible. Finding optimal cutting plane position is demanding and depend also on a frequency interval of interest.

The proposed hybrid approach is universal and not limited to the use of FMM or FEM. It could be applied to any set of methods suitable for the calculation of scattering matrices. For instance, FMM with BEM or MMP, FEM with BEM or MMP etc.

ACKNOWLEDGMENT

Special thanks to Nikolay Komarevskiy from ETH Zurich, Institute of Electromagnetic Fields (IFH) for discussions and good advices. The work is done under Swiss Science Foundation, Project 20021_143908.

REFERENCES

1. Hiptmair, R., "Finite elements in computational electromagnetism," *Acta Numerica*, 237–339, 2002.
2. Li, L. F., "New formulation of the fourier modal method for crossed surface-relief gratings," *J. Opt. Soc. Am. A*, Vol. 14, 2758–2767, 1997.
3. Tikhodeev, S. G., A. L. Yablonskii, E. A. Muljarov, N. A. Gippius, and T. Ishihara, "Quasiguided modes and optical properties of photonic crystal slabs," *Phys. Rev. B*, Vol. 66, No. 4, 045102, 2002.
4. Christ, A., T. Zentgraf, J. Kuhl, S. G. Tikhodeev, N. A. Gippius, and H. Giessen, "Optical properties of planar metallic photonic crystal structures: Experiment and theory," *Phys. Rev. B*, Vol. 70, No. 3, 125113, Sep. 2004.
5. Hafner, Ch. and R. Ballisti, "The multiple multipole method (MMP)," *Compel — The International Journal for Computation and Mathematics in Electrical and Electronic Engineering*, Vol. 2, No. 1, 1–7, 1983.
6. Talebi, N., M. Shahabadi, and Ch. Hafner, "Analysis of a lossy microring using the generalized multipole technique," *Progress In Electromagnetics Research*, Vol. 66, 287–299, 2006.
7. Sannomiya, T. and Ch. Hafner, "Multiple multipole program modelling for nano plasmonic sensors," *Journal of Computational and Theoretical Nanoscience*, Vol. 7, 1587–1595, 2010.
8. Yee, K. S., "Numerical solution of initial boundary value problems involving Maxwell's equations in isotropic media," *IEEE Transactions on Antennas and Propagation*, Vol. 14, 302–307, 1966.
9. Shlager, K. L. and J. B. Schneider, "A selective survey of the finite-difference time-domain literature," *IEEE Antennas and Propagation Magazine*, Vol. 37, No. 4, 39–57, 1995.
10. Kagami, S. and I. Fukai, "Application of boundary-element method to electromagnetic field problems," *IEEE Transactions on Microwave Theory and Techniques*, Vol. 32, No. 4, 455–461, 1984.

11. Buffa, A., M. Costabel, and C. Schwab, "Boundary element methods for Maxwells equations on non-smooth domains," *Numer. Math.*, Vol. 92, 679–710, 2002.
12. Komarevskiy, N., V. Shklover, L. Braginsky, and Ch. Hafner, "Ultrasensitive switching between resonant reflection and absorption in periodic gratings," *Progress In Electromagnetics Research*, Vol. 139, 799–819, 2013.
13. Deceglie, M. G., V. E. Ferry, A. Paul Alivisatos, and H. A. Atwater, "Design of nanostructured solar cells using coupled optical and electrical modeling," *Nano Lett.*, Vol. 12, 2894–2900, 2012.
14. Wilson, E. L. and R. E. Nickell, "Application of the finite element method to heat conduction analysis," *Nuclear Engineering and Design*, Vol. 4, 276–286, 1966.
15. Petyt, M., J. Lea, and G. H. Koopmann, "A finite element method for determining the acoustic modes of irregular shaped cavities," *Journal of Sound and Vibration*, Vol. 45, 495–502, 1976.
16. Ko, D. Y. K. and J. C. Inkson, "Matrix method for tunneling in heterostructures: Resonant tunneling in multilayer systems," *Phys. Rev. B*, Vol. 38, No. 14, 9945–9951, 1988.